

# Chapter 10

## Vacuum System

### 10.1 LER Vacuum System

This section discusses the vacuum system design for the LER regular arc sections, which occupy 2200 m out of the 3000 m circumference. The remaining parts of the LER are four 200 m long straight sections. One straight section is dedicated to beam collision and the interaction region for physics experiments. The others are reserved for beam injection, RF cavities and wiggler magnets.

#### 10.1.1 LER System Considerations

Copper has been chosen as the vacuum duct material for its ability to withstand a high peak heat load, and to shield radiation from the beam. The beam duct has a circular cross section with an outer diameter of 106 mm. The wall thickness is 6 mm, which is sufficient for radiation shielding, while being appropriate for fabrication. The expected radiation dose outside vacuum duct is well below  $1 \times 10^8$  rad/year. The grade of copper is ASM C10100 (oxygen-free electronic copper) for vacuum surface, and C10200 (oxygen-free copper) elsewhere. Vacuum flanges are made of stainless steel AISI304. The magnetic permeability of stainless steel must be less than 1.2 so as not to magnetically disturb the beam.

The LER stores a positron beam having an energy of 3.5 GeV at a maximum current of 2.6 A. The bending radius of a dipole magnet is 16.31 m. The total power of synchrotron radiation will be 2117.1 kW, and its critical energy 5.84 keV. As an option, there is a plan to add wiggler magnets to the LER, so that its radiation damping time will equal that of the HER. When this is done, the total radiation power will be increased to 3817.2 kW (i.e. the same as HER).

The cooling capacity of the refrigerators for the TRISTAN vacuum chamber has

been 4464 kW. This capacity must be increased to  $3817.2 \times 2 = 7634.4$  kW. A total water flow rate of 1600  $\ell/\text{min}$  is available for each quadrant of two rings, whose combined length is 1500 m. To ensure a 15  $\ell/\text{min}$  flow of water which is required based on thermal calculations, one loop of peripheral circulation must cover about 10 m of the vacuum duct.

With a bending angle of  $3.214^\circ$  per dipole magnet, the linear heat load on the chamber wall is estimated to be between  $27.6 \text{ W m}^{-1}$  and  $14.8 \text{ kW m}^{-1}$ . Due to this horizontally localized heat, the temperature of the beam duct rises locally to  $120^\circ \text{ C}$ . Consequently, a high local strain of  $-0.15\%$  appears along the  $z$  direction. Applying a  $0.15\%$  strain over  $10^8$  cycles does not cause cracking on a half or quarter tempered OFC [1]. However, localized heating will lead to an annealing of the material, which can reduce the local mechanical strength. Annealed OFC can still withstand  $10^4$  cycles of a  $0.5\%$  deformation at  $150^\circ \text{ C}$  [2]. However, it is preferred to keep the local temperature below  $140^\circ \text{ C}$  at KEKB.

The gas desorption induced by synchrotron radiation, and its implications to the expected vacuum pressure, have been analyzed. The desorption rate is proportional to the number of incident photons. The linear photon density ( $N$ ) averaged over the entire LER arc (2200 m) is  $3.3 \times 10^{18} \text{ photons s}^{-1}\text{m}^{-1}$  for the LER. While the desorption coefficient  $\eta$  (molecules per photon) is dependent on the surface finish, roughly it is decreased with the accumulated photon dose. An average pressure  $P$  (Torr) is given by

$$P = K^{-1}\eta N/Sd = 0.1\eta/Sd, \quad (10.1)$$

where  $K$  is a unit conversion coefficient ( $= 3.3 \times 10^{19} \text{ molecules Torr}^{-1}\ell^{-1}$ ) and  $Sd$  is the distributed pumping speed in units of  $\ell \text{ s}^{-1}\text{m}^{-1}$ .

The pressure-level goal to achieve at KEKB in the presence of the beam is  $1 \times 10^{-9}$  Torr. Our vacuum system has been designed such that this is achieved when  $\eta$  reaches  $10^{-6}$ . At storage rings an assumption is often made that  $\eta = 10^{-5}$ . However, this requires an enormous pumping speed, which will be impractical at KEKB. An  $\eta$  value of  $10^{-6}$  is considered to be realistic after a reasonable running time and the resultant beam dose ( $\sim 1000 \text{ Ah}$ ) at KEKB. The required pumping speed under this condition is  $100 \ell\text{s}^{-1}\text{m}^{-1}$ .

Small bunch sizes and the high current of KEKB place additional requirements on the vacuum system design. The size of any steps of the vacuum duct (i.e. discontinuity of the inner surface shape) may not exceed 0.5 mm. Pumping slots must be backed up by a grid, so that the penetration of wake fields, which causes a heat-up of the pumping elements, is reduced. Bellows and flange connections should be protected from direct synchrotron radiation hits. This will be accomplished by using suitably shaped masks

in the vacuum duct. However, the height of a mask must be lower than 5 mm. In this regard, a large bend angle in the LER creates a challenging condition for the bellows immediately downstream of the dipole magnets.

### 10.1.2 LER Vacuum System Components

Our design does not adopt an ante-chamber scheme. In the LER the synchrotron radiation is simply distributed on the duct wall. In this configuration it is preferred to distribute pumping slots along the beam duct.

An issue here is how to cope with possible beam-induced radiation onto the vacuum pumps. Unfortunately no reliable estimation is available concerning the magnitude of the radiation that propagates through pumping slots. Consequently, the vacuum system design must be prepared for an unexpectedly high power penetration. This will be done by making it possible to install a second grid between the slots and pumping elements.

All of the pumping elements are, therefore, attached to the vacuum duct via a flange connection to a pumping port. With the relatively large vacuum conductance of the beam duct ( $98 \text{ } \ell\text{s}^{-1}$ ), it has been shown that a distributed pumping speed of  $100 \text{ } \ell\text{s}^{-1}\text{m}^{-1}$  should be possible by installing pumps having a capacity of  $100 \text{ } \ell\text{s}^{-1}$  every 1 m. In practice, because of the presence of magnets, such a uniform distribution of the vacuum pumps cannot always be realized. This causes about a 20% reduction of the distributed pumping speed. Figure 10.1 shows the basic arrangement of the vacuum duct in a regular cell. A calculation of the distributed pumping speed for a part of the regular cell is shown in Figure 10.2.

In the current design three types of beam ducts will be fabricated for the LER. The first is the “B chamber” which is used with dipole bend magnets. It has a cooling channel and a mask, as well as pumping ports. The second is the “Q chamber” which is used for quadrupole magnets. It includes a beam position monitor and a mask, but no pumping port. The cooling channels are welded on both sides. The third is a straight “S chamber” which has a cooling channel, a mask and pumping ports. Examples of those chambers are shown in Figures 10.3, 10.4 and 10.5.

A typical cross section of a LER vacuum duct is shown in Figure 10.6. Two water channels are electron-beam welded to the outside of the S chamber in a symmetric way. One of the beam-based alignment techniques of magnets planned at KEKB will utilize an active modulation of the excitation of the quadrupole and sextupole magnets. The symmetric arrangement of water channels causes an eddy current to be induced with a good left-right symmetry. This symmetry helps analyze the data without having to make corrections for asymmetric systematic effects.

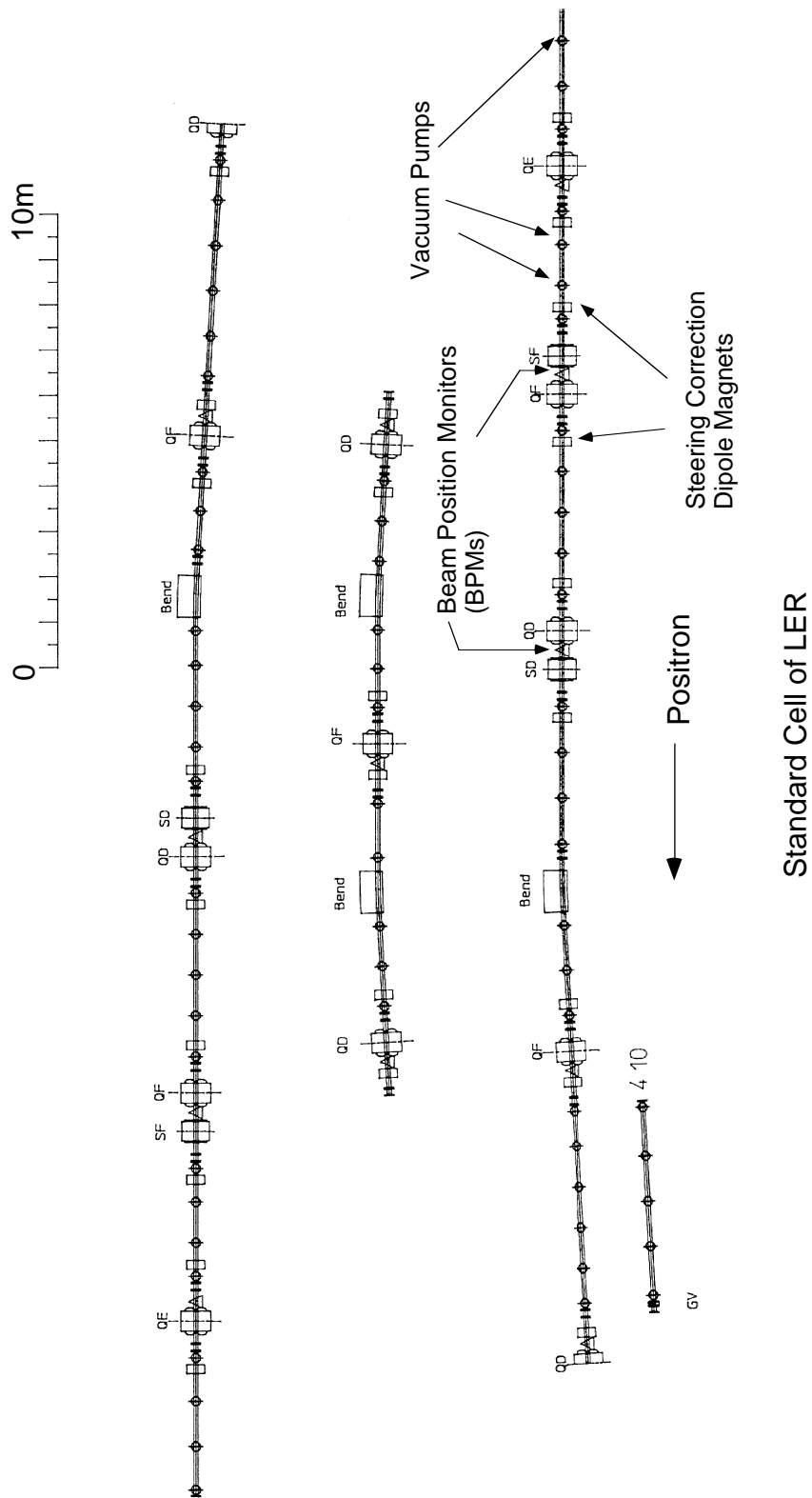


Figure 10.1: Basic layout of the vacuum duct in a LER regular cell.

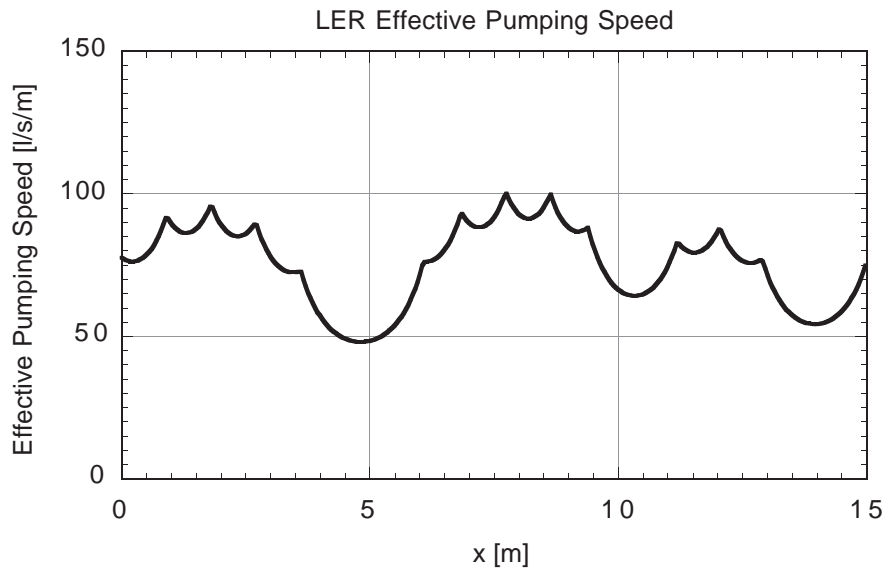


Figure 10.2: Expected pressure profile along the beam direction in the LER.

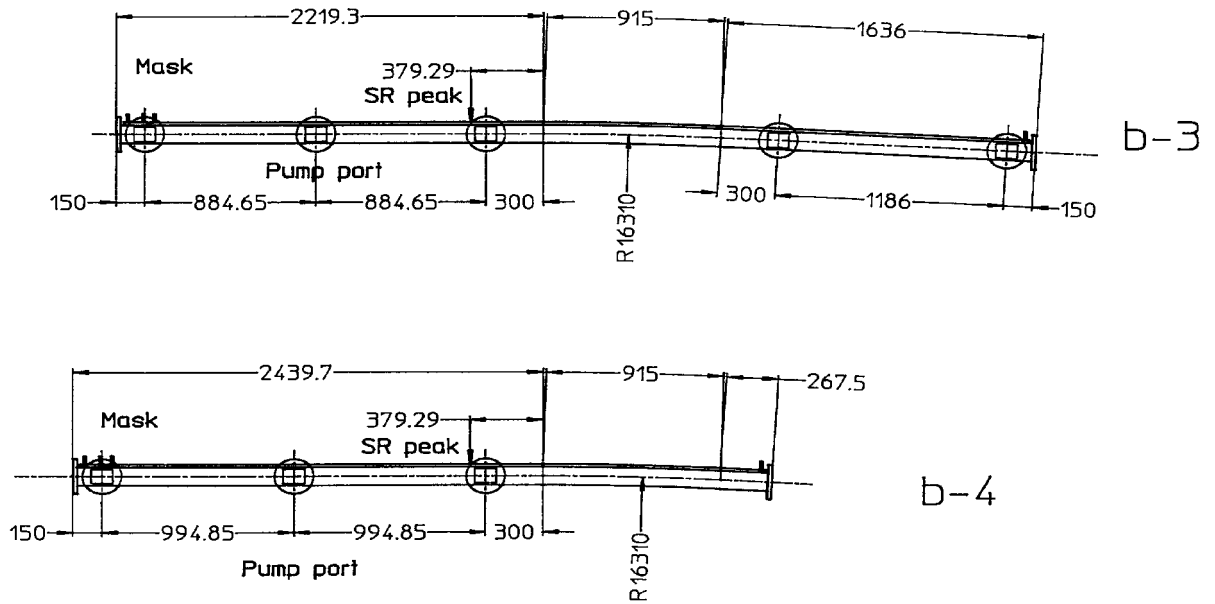


Figure 10.3: An example of the “B chamber” for the LER.

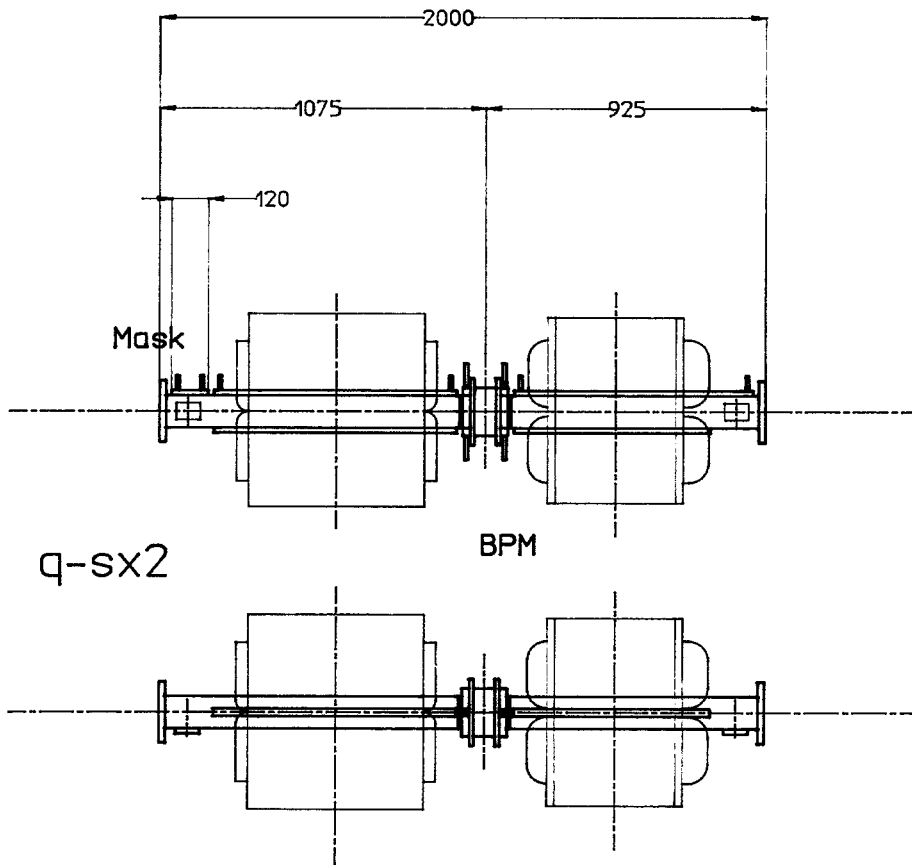


Figure 10.4: An example of the “Q chamber” for the LER.

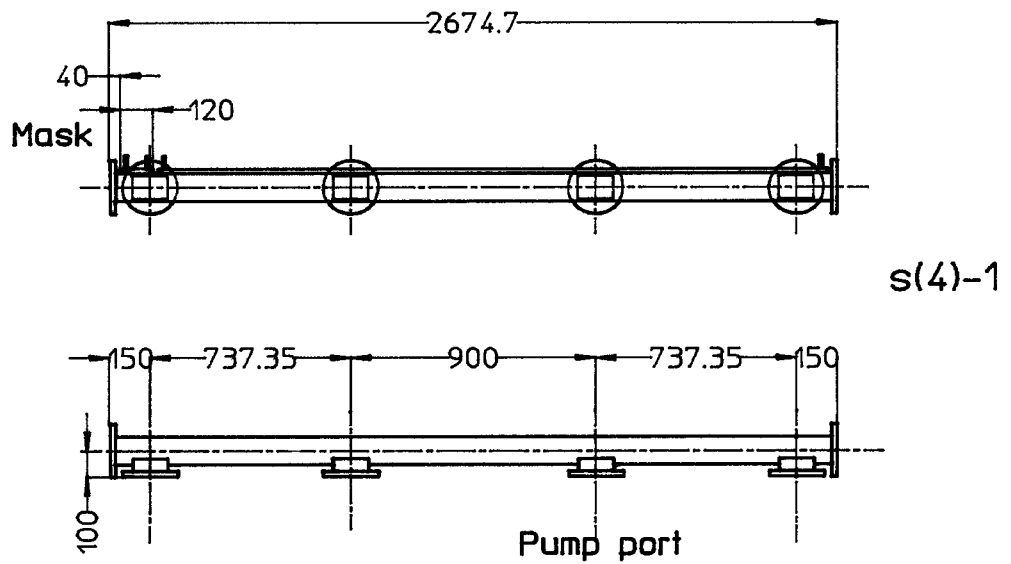


Figure 10.5: An example of the “S chamber” for the LER.

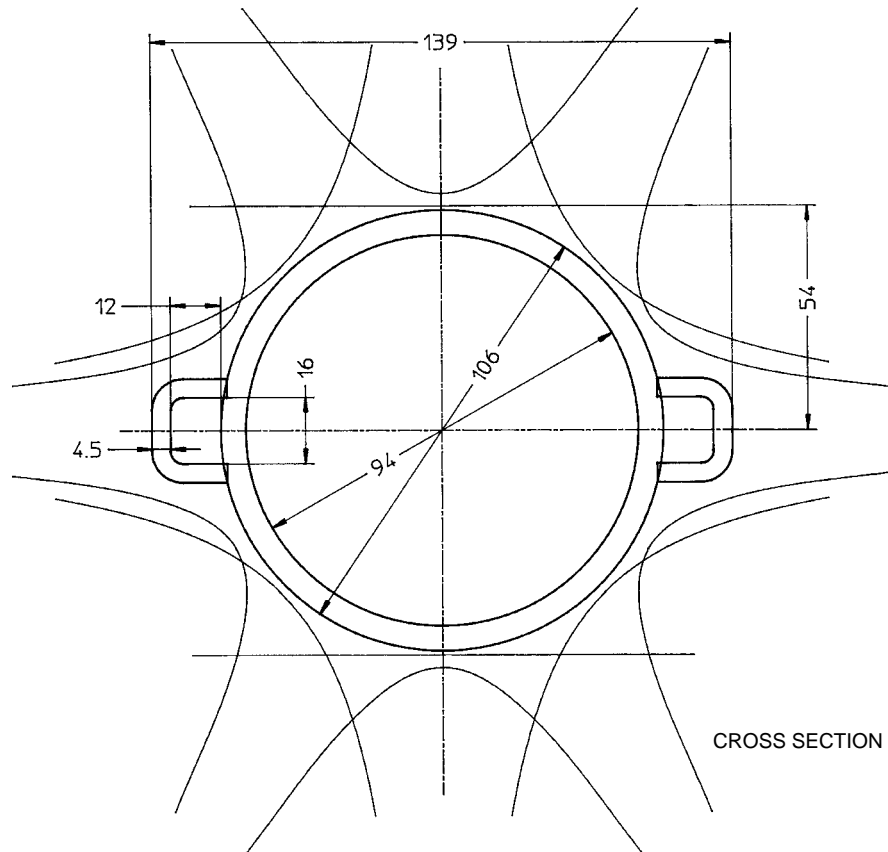


Figure 10.6: Cross section of an arc vacuum chamber for the LER. Two cooling water channels are symmetrically arranged. Outlines of the pole faces of quadrupole and sextupole magnets are also shown.

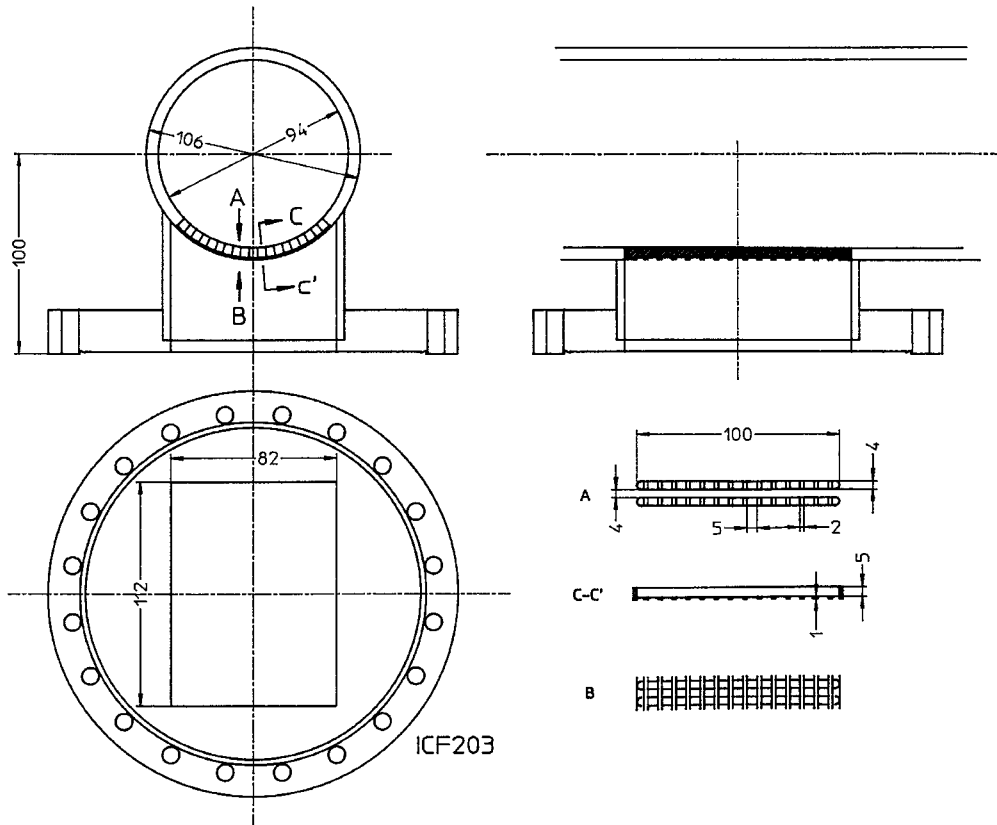


Figure 10.7: Structure of the LER pumping port and slots.

Figure 10.7 shows the structure of a pumping port and slots. The vacuum conductance of the slots of the port has been designed to be greater than  $200 \text{ } \ell\text{s}^{-1}$ . By using a  $200 \text{ } \ell\text{s}^{-1}$  NEG or a  $200 \text{ } \ell\text{s}^{-1}$  ion pump, a pumping speed of  $100 \text{ } \ell\text{s}^{-1}$  per port is expected to be achieved.

While the primary pumps comprise of NEG cartridges, secondary pumping is provided by ion pumps, which are installed every 10 m. Those ion pumps are required for operating the NEGs. They are also expected to bring the pressure down to about  $10^{-7}$  Torr during the initial pump down before the first activation of the NEGs.

An oxide layer on the duct inner surface contains a large amount of carbon compositions, which are released as CO and CO<sub>2</sub> in desorption. To avoid the necessity of frequent conditioning of the NEG during commissioning, it is necessary to remove this first oxide layer and to produce a new oxide layer that is free of carbon. This treatment will be done using a commercially available chemical cleaner containing H<sub>2</sub>O<sub>2</sub> and H<sub>2</sub>SO<sub>4</sub>, or by applying a standard acid etch with H<sub>2</sub>SO<sub>4</sub>, HNO<sub>3</sub>, HCl, and water. The effect of each cleaning is shown in Figure 10.8.

The bellows and flanges must be protected from direct exposure to synchrotron light. For this purpose a mask structure is embedded at one end of each vacuum duct unit. A schematic design diagram of a mask is shown in Figure 10.11. A mask



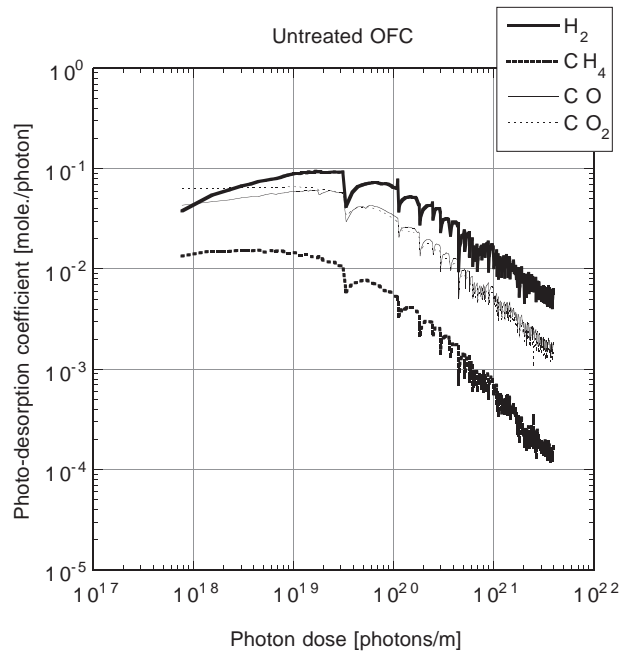


Figure 10.8: Measured photo desorption rate of hydrogen, water, carbon mono oxide and carbon di-oxide as function of accumulated photon doze. In this case, the copper material is not treated by chemical cleaner nor by acid etching.

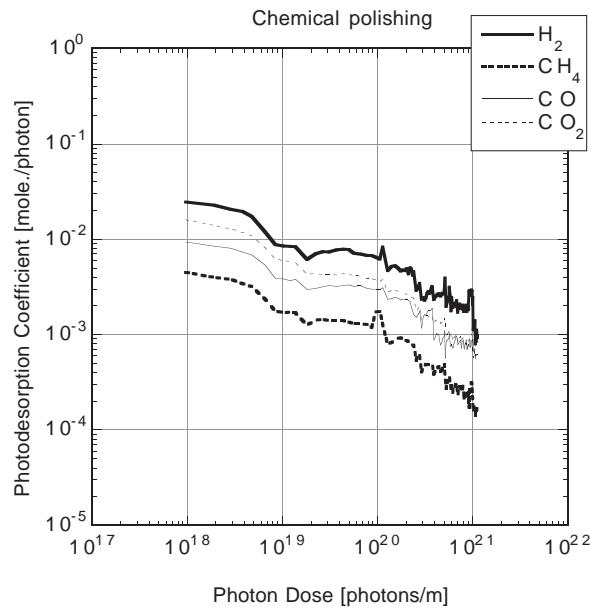


Figure 10.9: Measured photo desorption rate from a copper sample which has been cleaned by chemical cleaner.

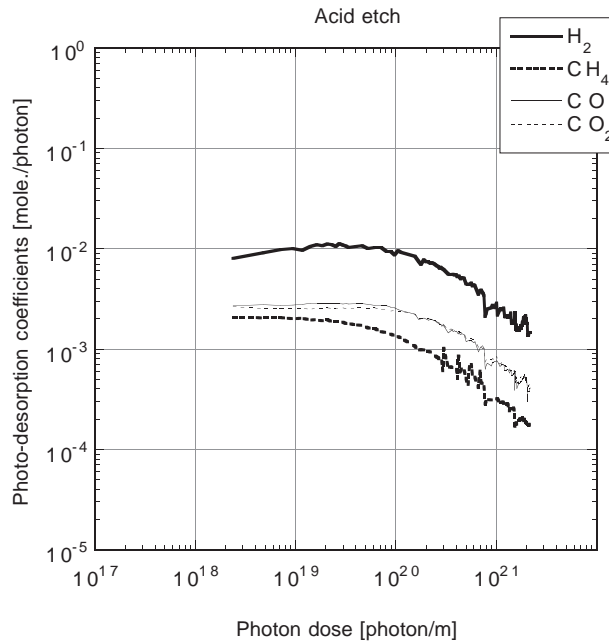


Figure 10.10: Measured photo desorption rate from a copper sample which has been processed by standard acid etching.

receives a larger amount of heat than the surrounding wall. The most stringent case is a 1.41 kW heat load for a 12 cm mask. The maximum temperature will reach about 130° C. This level of temperature rise is not considered to be problematic.

Button electrodes of the beam position monitor (BPM) unit are blazed on a copper block. The locations of the BPMs in a regular cell are shown in Figure 10.1. The design of the BPM blocks is discussed in chapter 11. The heat load due to synchrotron radiation depends on the location of individual BPMs. The heat deformation of the BPM units has been estimated. About one hundred BPMs will have their pickup feed-through assemblies shifted by 10 to 20  $\mu\text{m}$ . However, if the shift of four electrodes in a BPM unit occurs in a symmetric way, the net effect does not cause an apparent shift of measured beam position. It only causes a very small change of the BPM sensitivity.

Bellows of two different designs (Type A and Type B) are being considered for the LER, as shown in Figures 10.12 (Type-A) and 10.13 (Type-B). In a Type-A bellows a tube seal is used as the RF contact. The seal follows the possible deformation of the bellows unit. A Type-B bellows has a finger contact. The loss factor of the Type-B bellows is expected to be smaller than that of Type-A. However, since a Type-B bellows has long slot gaps between the fingers, field penetration through those gaps is a potential problem. It appears to be difficult to plug those gaps while maintaining good mechanical flexibility. A possible design solution is to adopt a Type-B bellows,

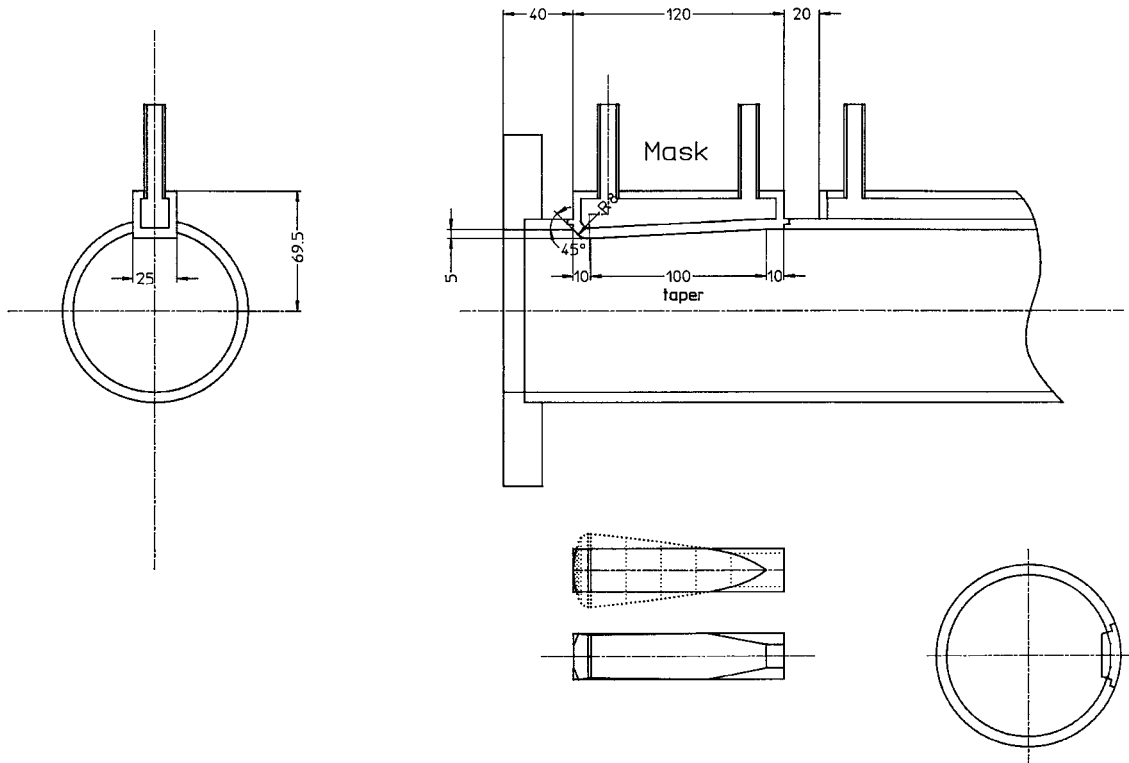


Figure 10.11: Cross section and side view of a synchrotron radiation mask within a LER vacuum duct.

but to limit the slot length exposed to the bunch to be  $\sim 1/2$  of the stroke of the bellows.

The connection with standard conflat flanges will leave a gap between the gasket and the flange where the beam field can be trapped. The estimated energy loss at a connection is 635 W. This causes a heating of the flanges. To avoid this situation, beam ducts must be connected without any gaps at the flange. In the proposed design, an aluminum ring is inserted between flange faces to fill the gap. A vacuum seal is made outside of the ring using Helicoflex. The structure based on this idea is shown in Figure 10.14.

## 10.2 HER Vacuum System

### 10.2.1 HER System Considerations

Overall, the HER ring has a structure similar to that of the LER. An arc with regular cells has a total length of 2200 m. One straight section is intersecting with LER for collision, two are used for cavities. The last straight section includes a cross-over with the LER as well as an injection complex.

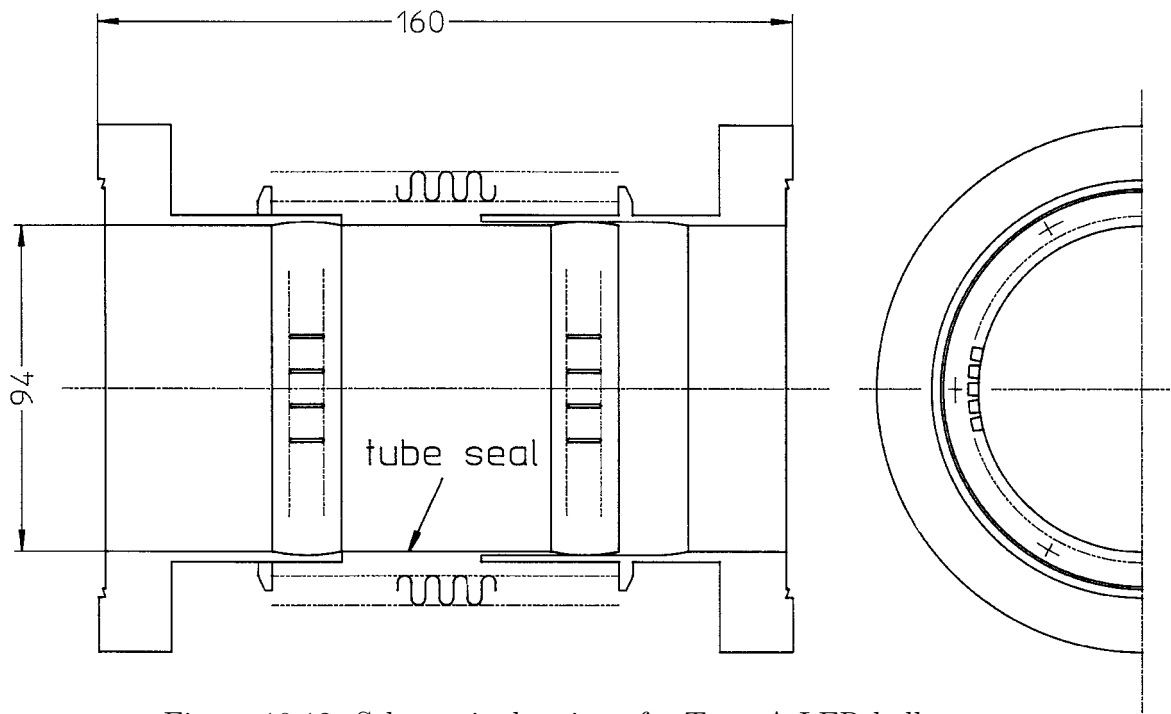


Figure 10.12: Schematic drawing of a Type-A LER bellows.

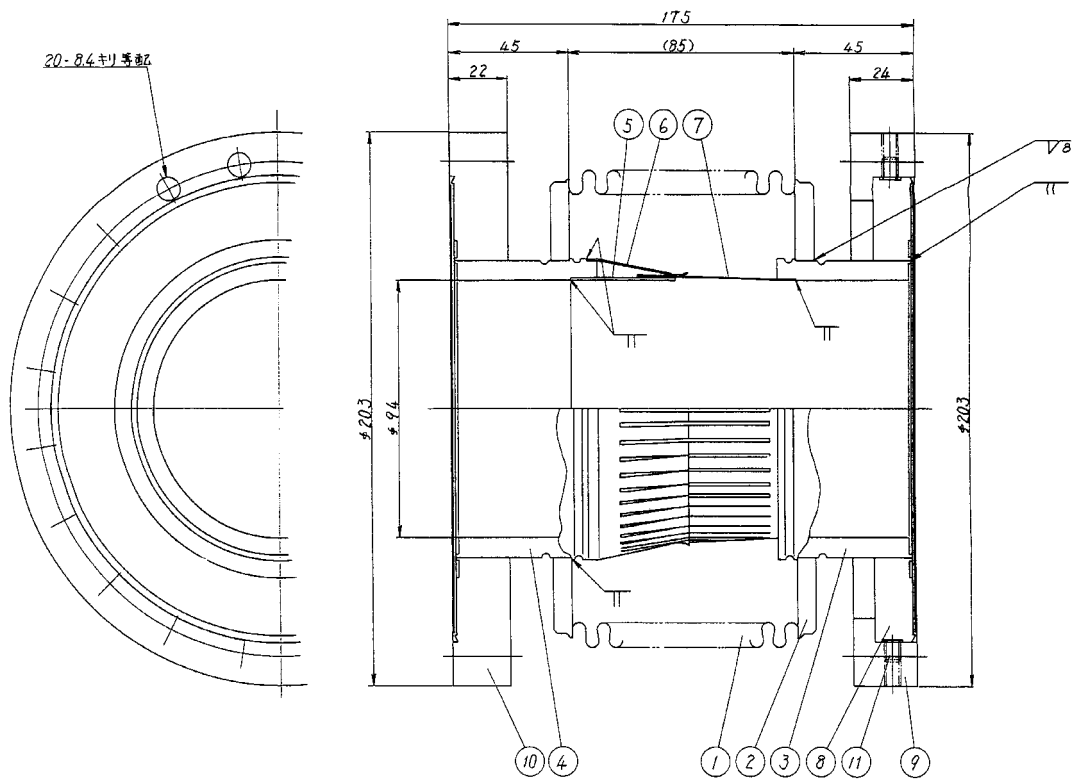


Figure 10.13: A schematic drawing of a Type-B LER bellows.

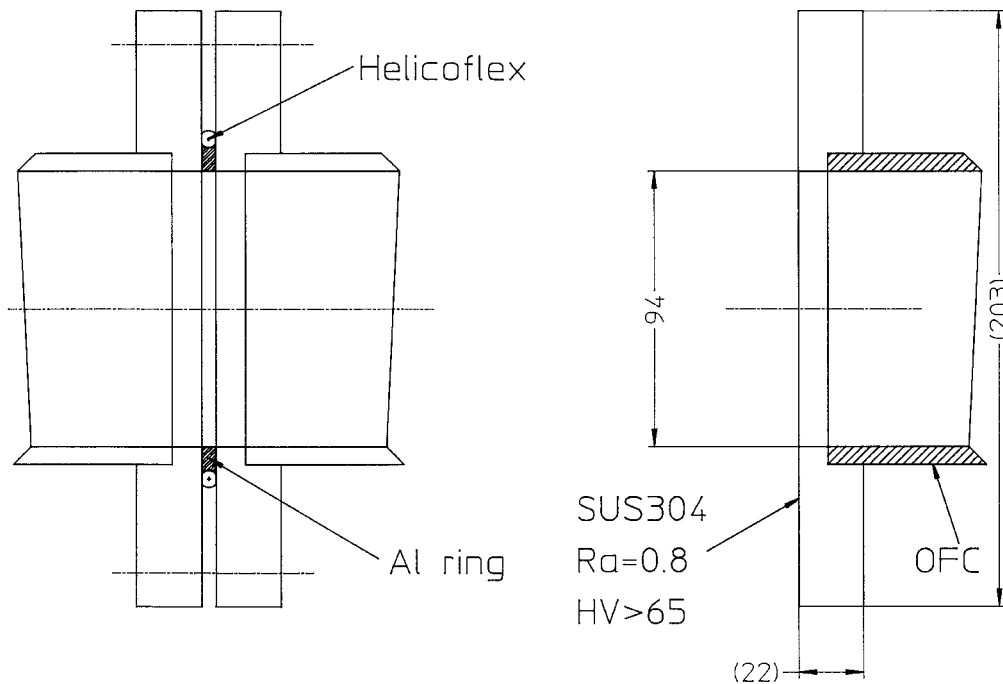


Figure 10.14: Vacuum sealing using Helicoflex.

As shown in Figure 10.15, the cross section of the HER beam duct has a racetrack shape with a 58 mm half width and  $r = 31$  mm (outer curvature) with a thickness of 6 mm. The vacuum duct will be made of copper.

The HER stores the electron beam of  $E = 8$  GeV at a maximum current of  $I = 1.1$  A. The orbit bend radius in a dipole magnet is 104.46 m. The total power of synchrotron radiation is 3817.2 kW with a critical energy of 10.9 keV. Synchrotron radiation will hit the wall of the beam duct within a dipole magnet. The maximum linear heat load on the chamber wall in the arc is  $5.8 \text{ kW m}^{-1}$ . This heat load allows the use of an aluminum alloy.

The linear photon density in the HER averaged over the arc (2200 m) is expected to be  $3.2 \times 10^{18} \text{ photons s}^{-1} \text{ m}^{-1}$ . This situation is quite similar to that of the LER. Consequently, the distributed pumping speed in the HER is also  $100 \text{ l s}^{-1} \text{ m}^{-1}$ .

Since the beam current is lower than the LER, expected wake field problems at HER are not so serious as in the LER. A beam duct is pumped through side slots (backed up with grid) and NEG strips are used as the distributed pump.

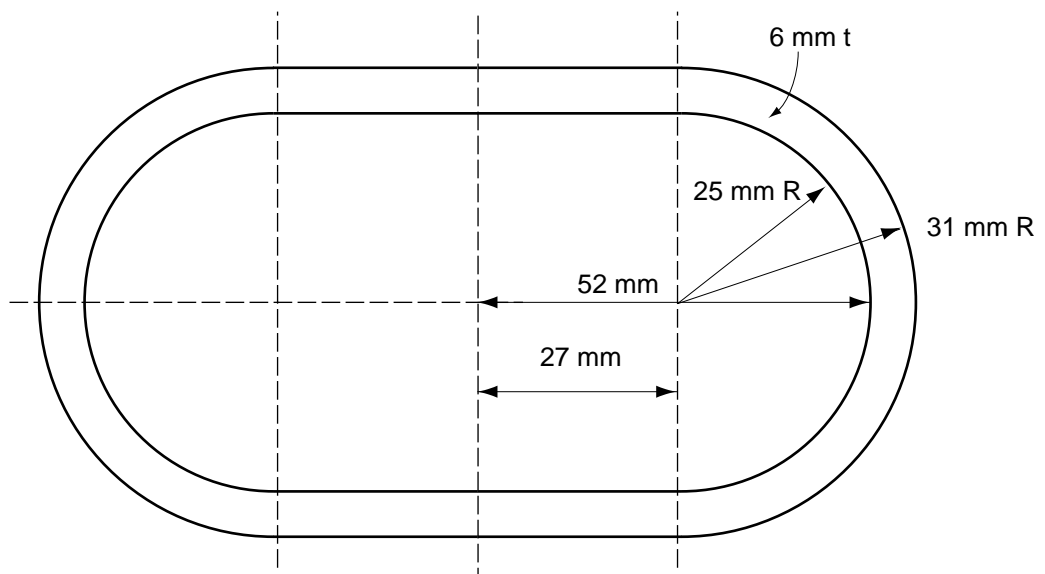


Figure 10.15: Cross section view of the arc vacuum chamber for the HER.

# Bibliography

- [1] Private communication with Hitachi Works, Co. Ltd.
- [2] Private communication with Hitachi Cable, Co. Ltd.